



HAL
open science

Cortical sensorimotor activity in the execution and suppression of discrete and rhythmic movements

Mario Hervault, Pier-Giorgio Zanone, Jean-Christophe Buisson, Raoul Huys

► **To cite this version:**

Mario Hervault, Pier-Giorgio Zanone, Jean-Christophe Buisson, Raoul Huys. Cortical sensorimotor activity in the execution and suppression of discrete and rhythmic movements. *Scientific Reports*, 2021, 11 (1), pp.Article number: 22364. 10.1038/s41598-021-01368-2 . hal-03448514

HAL Id: hal-03448514

<https://hal.science/hal-03448514>

Submitted on 27 Nov 2021

HAL is a multi-disciplinary open access archive for the deposit and dissemination of scientific research documents, whether they are published or not. The documents may come from teaching and research institutions in France or abroad, or from public or private research centers.

L'archive ouverte pluridisciplinaire **HAL**, est destinée au dépôt et à la diffusion de documents scientifiques de niveau recherche, publiés ou non, émanant des établissements d'enseignement et de recherche français ou étrangers, des laboratoires publics ou privés.

1 **Cortical sensorimotor activity in the execution and suppression of**
2 **discrete and rhythmic movements**

3

4 Mario Hervault^{1*}, Pier-Giorgio Zanone¹, Jean-Christophe Buisson², Raoul Huys¹

5 ¹ Centre de Recherche Cerveau et Cognition – UMR 5549 CNRS – Université

6 Toulouse 3 Paul Sabatier

7 ² Institut de Recherche en Informatique de Toulouse – UMR 5505 CNRS –

8 Université Toulouse 3 Paul Sabatier

9

10 ***Corresponding author:**

11 Mario Hervault

12 CNRS CERCO UMR 5549, Pavillon Baudot CHU Purpan, BP 25202 - 31052

13 TOULOUSE CEDEX

14 mario.hervault@cnrs.fr

15

16 **Competing interests**

17 The author(s) declare no competing interests.

18

19 **Author Contributions**

20 M.H., PG.Z., J.C.B. and R.H. are responsible for the study concept and design.

21 M.H. acquired the data. The analysis and interpretation of data were carried

22 out by M.H., PG.Z. and R.H. The manuscript was drafted by M.H., PG.Z. and

23 R.H. All authors gave approval of the final submitted version.

24 Abstract

25 Although the engagement of sensorimotor cortices in movement is well docu-
26 mented, the functional relevance of brain activity patterns remains ambigu-
27 ous. Especially, the cortical engagement specific to the pre-, within-, and
28 post-movement periods is poorly understood. The present study addressed
29 this issue by examining sensorimotor EEG activity during the performance as
30 well as STOP-signal cued suppression of movements pertaining to two distinct
31 classes, namely, discrete vs. ongoing rhythmic movements. Our findings indi-
32 cate that the lateralized readiness potential (LRP), which is classically used as
33 a marker of pre-movement processing, indexes multiple pre- and in- move-
34 ment-related brain dynamics in a movement-class dependent fashion. In- and
35 post-movement event-related (de)synchronization (ERD/ERS) observed in the
36 Mu (8-13 Hz) and Beta (15-30 Hz) frequency ranges were associated with es-
37 timated brain sources in both motor and somatosensory cortical areas. Not-
38 withstanding, Beta ERS occurred earlier following cancelled than actually per-
39 formed movements. In contrast, Mu power did not vary. Whereas Beta power
40 may reflect the evaluation of the sensory predicted outcome, Mu power
41 might engage in linking perception to action. Additionally, the rhythmic
42 movement forced stop (only) showed a post-movement Mu/Beta rebound,
43 which might reflect an active "clearing-out" of the motor plan and its feed-
44 back-based online control. Overall, the present study supports the notion that
45 sensorimotor EEG modulations are key markers to investigate control or ex-
46 ecutive processes, here initiation and inhibition, which are exerted when per-
47 forming distinct movement classes.

48 Keywords

49 PMBR, inhibitory control, oscillations, time-frequency, source localization

50 **Introduction**

51 It has long been known that when performing a voluntary action, cortical sensorimotor areas are engaged in movement planning, execution and
52 online control ¹. Most corresponding accumulated knowledge has been acquired in the context of the generation of discrete movement, which constitute an important, but not sole class of movements that humans can perform
53
54 ². Consequently, two aspects of action control and its neural sensorimotor underpinnings are strongly under-represented. On the one hand, we know little
55 about cortical sensorimotor engagement related to movement suppression, even though both movement generation *and* suppression are commonplace
56
57 in our interaction with the environment ³. On the other hand, previous investigations of neural activity when suppressing movements have focused exclusively on short-lived discrete movements and have then ignored the case of
58
59 *ongoing-rhythmic* movement suppression, which is also crucial in action control ⁴⁻⁷. The few studies at hand on sensorimotor activity related to action suppression have dealt with prepared discrete movements ⁸⁻¹¹, discrete movements sequence ^{12,13} or isometric force exertion ^{14,15}. Kinematically, discrete
60
61 actions are delimited by moments without movement (i.e., with zero velocity and acceleration), such as grasping an object. In contrast, continuous actions, such as walking, lack recognizable endpoints and are typically considered
62
63 rhythmic if they constitute (periodic) repetitions of particular events ². Motor control encompasses both action classes, which differ not only regarding their kinematics ¹⁶ but also in terms of movement dynamics and control processes
64
65 ^{17,18}, as well as of corresponding brain engagement ¹⁹. Indeed, the neural structures associated with controlling discrete and rhythmic actions differ considerably ¹⁹⁻²¹, due to different timing and initiation mechanisms ^{17,20}. Additionally, integrating in- and post-movement sensory information shows distinct dynamics between discrete and rhythmic action classes ^{22,23}, which may involve open- and closed-loop control, respectively. As sensorimotor EEG activity has been linked to movement-related sensory integration in the framework of forward internal models of motor control (see below), its investigation and comparison in both movement classes appears to be crucial.

82 The present study aims to help providing a more complete picture of
83 the cortical sensorimotor activity underlying action control through the study
84 of both the performance *and* suppression of movements belonging to two
85 fundamentally distinct classes, discrete *and* rhythmic movements. EEG activ-
86 ity over sensorimotor areas was analyzed in terms of the lateralized readi-
87 ness potential (LRP) and event-related (de)synchronization (ERS/D) of Mu (8 -
88 13 Hz) and Beta (15 - 30 Hz) cortical oscillations. In addition, a second objec-
89 tive was to provide new insights into understanding the functional relevance
90 of these movement-related neural sensorimotor activities with regard to ac-
91 tion executive control.

92 Prior work has established standard non-invasive methods to explore
93 movement-related brain activity. When recording scalp EEG, the LRP is be-
94 lieved to reflect the central response preparation within the primary motor
95 cortex (M1) that control the movement ²⁴. As for brain oscillations, a well-de-
96 fined pattern of activity has been described during and after movement exe-
97 cution in Mu and Beta rhythms. This pattern is characterized by an ERD asso-
98 ciated with the movement's execution, followed by an ERS subsequent to the
99 movement stop ²⁵. This ERD/ERS pattern has been recorded over sensorimo-
100 tor areas for several (contrasting) movement conditions, including self-paced
101 and stimulus-triggered movements ^{26,27}, real and imagined movements ²⁸, as
102 well as discrete short responses and lasting rhythmic movements ^{29,30}. Espe-
103 cially, the cortical ERD/ERS dynamics were clearly observed for each move-
104 ment cycle in the case of low-frequency movement repetition (< 1 Hz), that
105 is, when the repetition was most likely due to a concatenation of discrete
106 movements. In contrast, it transformed into a sustained ERD during higher-
107 frequency movement repetition, that is, when the movements were truly
108 rhythmic ³⁰⁻³².

109 Despite the large number of studies reporting these movement-related
110 neurophysiological modulations, their functional relevance remains debated.
111 The LRP is thought to reflect the pre-movement M1 engagement as a final
112 pathway for the central generation of movement, that is, the downstream
113 specification of commands to the peripheral motor structures ³³. Accordingly,
114 LRP is massively used as an index of movement initiation when triggering dis-

115 crete movement across multiple simple and choice reaction time tasks ^{34,35}. In
116 this context, LRP may follow a fixed-threshold dynamics, that is, the reaching
117 a threshold activation amplitude determines whether the response will be
118 triggered or not ^{36,37}. Based on the assumption that the reach of this threshold
119 discriminates successfully from failed cancellations of a prepared discrete
120 movement ³³, LRP has become a popular tool for investigating discrete action
121 inhibition ³⁸⁻⁴¹. When performing a continuous action, an external signal may
122 indicate the performer to speed up ⁴², continue ⁴³ or stop ^{6,12,42} the ongoing ac-
123 tion. In such cases, a new command specification might engage in the build-
124 ing up of the motor activity. However, the purported assignment of LRP to
125 pre-movement processing has led to its dereliction for investigating the vol-
126 untary modulation or suppression of an ongoing rhythmic movement. Indeed,
127 the very possibility of an LRP reduction has been ignored by the few studies
128 exploring rhythmic movement stopping ^{7,43}.

129 The Mu/Beta ERD reflects the desynchronization of an ensemble of cor-
130 tical neurons over sensorimotor brain areas. In contrast, the post-movement
131 Mu/Beta ERS reflects its neural resynchronization ⁴⁴. The Mu/Beta activity has
132 been initially suggested to echo a cortical idling state during "mental inactiv-
133 ity" ⁴⁵ or a "status quo" in maintaining the current sensorimotor or cognitive
134 state ⁴⁶. Although Mu and Beta tend to follow a similar pattern of activity and
135 can be mapped to a single dipole due to an overlap in their cortical sources,
136 recent evidence showed that they index distinct neurological functions ⁴⁷.
137 These functions, which are still debated, have been proposed in the frame-
138 work of forward internal models of motor control ⁴⁸, in which the sensory con-
139 sequences of movement are predicted (through forward models) and com-
140 pared to the actual sensory outcome. Indeed, the Mu rhythm has been con-
141 sidered as an alpha-like oscillation engaged in a "diffuse and distributed al-
142 pha system", in reference to the multiple ~10 Hz rhythms originating from in-
143 dependent brain sources ⁴⁹. Within this broad alpha system, the Mu rhythm
144 might reflect a perception-to-action translation ^{47,50}. Accordingly, Mu syn-
145 chronicity occurs when visual and auditory representations are converted into
146 action-based representations. The potential distinction between sub-frequen-
147 cies bands ⁴⁷ and the Mu involvement in inverse models ⁵¹ is still examined.

148 At any rate, the Mu rhythm is generally viewed as a correlate of the recipro-
149 cal interaction between motor and sensory cortices, this interaction being
150 crucial in the internal models controlling the action.

151 According to recent reviews ^{47,52}, the Beta ERD reflects movement
152 preparation, including the adjustments of motor commands and the anticipa-
153 tion of errors ⁵³. The Beta ERD modulation by movement uncertainty ⁵⁴ also
154 suggests that it plays a role in predicting the sensory consequences of the ac-
155 tion. The observation of an above-baseline ERS following movement, known
156 as the post-movement Beta rebound (PMBR), led to multiple hypotheses.
157 Beta oscillations could reflect the post-movement processing of sensory reaf-
158 ference ⁵⁵. Indeed, the occurrence of PMBR after passive movements ⁵⁶ or
159 when accompanying peripheral nerve stimulation ⁵⁷ is consistent with the
160 idea that PMBR originates in sensory feedback to the motor cortices. More
161 specifically, the PMBR was proposed to index the integration of sensory feed-
162 back to evaluate movement outcome, with any deviation from the forward-
163 predicted outcome leading to an update of the motor plan ⁴⁷. Alternatively,
164 PMBR could reflect the active inhibition of the motor cortex to terminate a
165 movement ⁵⁸. The observation of a single PMBR following a sequence of dis-
166 crete movements ^{13,59} and its association to movement parameters such as
167 accuracy, variability, and rate of force development ^{60,61} have been taken as
168 an argument for its involvement in the active inhibition of the motor cortex
169 following movement termination.

170 All in all, multiple interpretations have been put forth to explain neural
171 sensorimotor activity before, during and after a movement. Additionally, in
172 relation to the ERD/ERS pattern, the brain activation found over both pre-
173 (motor) and post-Rolandic (somatosensory) areas ^{50,52,62} contributes to blur
174 the numerous functional hypotheses. Still, experiments requiring both initia-
175 tion and suppression of movement have tried to provide new insight into the
176 functionality of the sensorimotor ERD/ERS by showing that its occurrence de-
177 pends on whether a movement is actually performed versus withheld ¹¹. The
178 cortical activity also differed between normal movement completion and
179 forced suppression ¹² and between quick and slow movement termination ¹⁴.
180 However, the characterization of the movement-related sensorimotor activity

181 suffers from large variation in the task parameters employed across studies
182 (e.g., task duration and movement amplitude), which alters the correspond-
183 ing neural activity, and has hampered the establishment of convincing func-
184 tional interpretations ¹⁵.

185 To complement our understanding of the movement-related neural
186 sensorimotor activity, the present study examined EEG activity when per-
187 forming a movement and suppressing it. EEG was recorded in the context of
188 two fundamental classes of movement: discrete and rhythmic ones. Using a
189 graphic tablet, we asked participants to initiate a discrete movement after a
190 GO stimulus and pursue a rhythmic movement after a CONTINUE stimulus. In-
191 frequently, a STOP signal following the primary stimulus indicated partici-
192 pants to cancel the prepared-discrete movement or to stop the ongoing-
193 rhythmic one. Firstly, in line with the interpretation of LRP as a sign of move-
194 ment preparation, we hypothesized its large amplitude following a GO stimu-
195 lus to contrast with its absence following a CONTINUE stimulus, and the STOP
196 signal occurrence to reduce its amplitude in the discrete experiment only.
197 Secondly, following the assumption that Mu and Beta rhythms encode recip-
198 rocal interactions between motor and sensory cortices to enable monitoring
199 of movement, we expected to observe a sustained Mu ERD during ongoing
200 rhythmic movement ³⁰, reflecting the closed-loop processing of sensory infor-
201 mation in the CONTINUE condition, and it to be aborted by movement sup-
202 pression in the STOP condition. In contrast, we expected to indifferently ob-
203 serve a transient Mu ERD/ERS in discrete completed, successfully cancelled,
204 and unsuccessfully cancelled actions, as the movement is controlled in an
205 open-loop fashion, and to observe a transient and sustained Beta ERD, re-
206 flecting motor activation, in the discrete and rhythmic condition, respectively.
207 Third, we anticipated a PMBR, reflecting the post-movement sensory "check",
208 to be visible after movement suppression in the rhythmic STOP ¹⁴ and the dis-
209 crete conditions, with differences between the discrete completed, success-
210 fully cancelled, and unsuccessfully cancelled actions, for the movement out-
211 come differs in each case ¹¹.

212 **Method**

213 ***Participants***

214 Fifteen healthy individuals (9 males, mean age 25 years, SD = 2.2)
215 served as voluntary participants. All were right-handed, as assessed by the
216 Edinburgh Handedness Inventory ⁶³, and had a normal or corrected-to-normal
217 vision. None of the participants reported a history of psychiatric or
218 neurological disorders. The study was conducted with the informed consent
219 of all participants according to the principles stated in the Declaration of
220 Helsinki, and the procedures were approved by the local research ethics
221 committee (Comité de Protection des Personnes Sud-Ouest et Outre-Mer II;
222 ID-RCB: 2020-A03215-34).

223 ***Procedures***

224 *Experimental procedures*

225 Participants performed two experiments that have been previously de-
226 scribed ⁴³, and for which details are provided in Appendix A. Briefly, both ex-
227 periments required participants to perform voluntary right-hand movements
228 on a graphic tablet using a stylus. In both experiments, the participants com-
229 pleted one practice block and 30 experimental blocks, each consisting of 20
230 trials. In the first experiment, visual GO stimuli called for the quick initiation
231 of discrete-swipe movements (GO_D condition). Following the primary GO stim-
232 ulus, a STOP signal was presented infrequently (in 25 % of trials, STOP_D con-
233 dition), indicating the participants to cancel the prepared movement, leading
234 to successful-STOP_D or fail-STOP_D trials. The experiment was designed follow-
235 ing the recent guideline for stop-signal tasks ⁶⁴. In the second experiment,
236 participants executed self-paced rhythmic movements; a visual CONTINUE
237 stimulus called for the continuation of a rhythmic movement (CONTINUE con-
238 dition). As in the first (discrete) experiment, infrequently (in 25 % of trials,
239 STOP_R condition), a STOP signal followed the primary CONTINUE stimulus to
240 order participants to stop the ongoing movement quickly. Following such
241 STOP trials, a rhythmic GO_R trial was added to reengage participants in the

242 rhythmic movement. In these GO_R trials, participants were instructed to tran-
243 sit from a static position to an oscillating movement as soon as the GO stimu-
244 lus (green or blue) was presented. In both the discrete and rhythmic experi-
245 ment, the minimal delay between two trials was 3500ms and the primary
246 stimulus occurrence varied randomly in a 500 ms window. As such, the two
247 experiments are close in design in terms of the stimuli properties and the ef-
248 fectors engaged in the movement production; their main difference consisted
249 in the movement type to perform and stop, namely prepared-discrete versus
250 ongoing-rhythmic movements.

251 *EEG recording and preprocessing*

252 Scalp EEG was recorded using an ActiveTwo system (BioSemi
253 Instrumentation, 64 electrodes) with a sampling rate of 2048 Hz. The EEG
254 electrodes were cautiously positioned based on four anatomical landmarks
255 (i.e., nasion, inion, and preauricular points) in accordance with the 5 % 10/20
256 international system ⁶⁵. Additional electrodes were placed below and above
257 each eye. The data were online referenced to the BioSemi CMS-DRL
258 reference. All offsets from the reference were kept below 15 mV. The EEG
259 data were filtered online with a frequency bandpass filter of 0.5-150 Hz. The
260 participant's arm was fixed on the table to restrain the movement to wrist
261 articulation and avoid muscular noise in the EEG signal due to substantial
262 contraction of the biceps and deltoid muscles. Continuous EEG data were
263 imported and preprocessed in bespoke scripts using functions from the
264 EEGLAB Matlab plugin ⁶⁶ :

- 265 • Visual inspection was used to remove channels with prominent
266 artifacts in the continuous EEG.
- 267 • The EEG data were then re-referenced to a common average.
- 268 • The data were partitioned into epochs of 3 s (locked to the primary
269 stimulus onset; }1000 ms to 2000 ms).
- 270 • Those epochs containing values exceeding the average across the
271 data segments by 5 SD were rejected.
- 272 • Scalp EEG data typically represent a mixture of activities originating
273 from brain sources that are not separable based on channel data

274 solely. Independent component analysis (ICA) ⁶⁷ can be applied to
275 identify statistically independent signal components (ICs) spatially
276 filtered from the 64 channels data. An ICA was applied to continuous
277 EEG data (concatenation of the EEG epochs) to identify 63 neural ICs
278 contributing to the observed scalp data. Using the ICLABEL classifier
279 ⁶⁸ over the 30 first ICs, components with less than 10% chance to
280 account for neural activity were considered as artifacts, and removed
281 from the EEG data structure, thus removing their contributions to the
282 observed EEG. The rejection was systematically verified by visual
283 inspection of component properties (time series, spectra, topography)
284 according to ICLABEL guidelines ⁶⁸.

285 Across all participants, these procedures led to the omission of 8.6 % of
286 the STOP trials in the discrete task (SD = 1.4 %) and 4.1 % of the rhythmic
287 STOP trials (SD = 1.9 %).

288 **Measures**

289 *Reaction times (RT)*

290 The behavioral results of these experiments have been published sepa-
291 rately ⁴³. Here and in the results section (below) we shortly present the be-
292 havioral measures that are essential to appreciate the main (EEG) results.

293 In the discrete experiment, RT_{GO} was calculated in the GO_D trials as the
294 time between the primary stimulus onset and the response onset; the latter
295 was defined as the moment the reach had exceeded 5 % of the Euclidean dis-
296 tance between the initial and furthest (i.e., end) position of the discrete-
297 movement response. As an inhibitory RT, each participant's RT_{STOP-D} was esti-
298 mated using the integrative method for stop-signal tasks ^{64,69}. In the rhythmic
299 experiment, the movement-related StopTime was calculated as the time
300 elapsed between the STOP signal onset and the end of the movement (i.e.,
301 null velocity). Each participant's RT_{STOP-R} , that is, the time between the STOP
302 signal onset and the onset of movement alteration, was computed by identi-
303 fying, within the StopTime, the first time point that the movement statistically
304 deviated from the set of uninterrupted movements in the phase space ⁴.

305 *Lateralized readiness potentials*

306 In each condition LRPs were computed (using customized scripts writ-
307 ten on Matlab) to assess the build-up of cortical motor activity following the
308 primary stimulus (GO or CONTINUE). To this end, the EEG time series locked
309 to the primary stimulus onset were averaged following the subtraction of a
310 -200 to 0 ms pre-stimulus period as a baseline. The LRP was then derived
311 from the difference between electrodes C3 (the electrode over the contralat-
312 eral motor cortex) and C4 (its ipsilateral counterpart). This was done for GO_D,
313 successful-STOP_D, and fail-STOP_D trials in the discrete task and CONTINUE and
314 STOP_R trials in the rhythmic one. As LRP is classically characterized by a neg-
315 ative deflection underlying motor preparation, LRP peak amplitude was de-
316 fined in each condition by looking for the minimum peak value following stim-
317 ulus onset (LRPs were 15 Hz low-pass filtered for the peak detection). A simi-
318 lar subtraction, that is, contralateral activity minus ipsilateral activity and
319 vice versa, was performed for each pair of scalp electrodes (e.g., F3 minus
320 F4, CP3 minus CP4 ...) in order to display the lateralized part of the EEG activ-
321 ity as a topography (Fig. 1).

322 *Mu and Beta time-frequency analysis*

323 First, a time-frequency decomposition was performed according to the
324 procedure described below, using the preprocessed EEG data from the C3
325 channel ^{44,70,71}. The resulting time-frequency maps are shown for each
326 experimental condition in Appendix B to provide a classical view of our data.

327 Second, a time-frequency analysis was performed with a focus on the
328 Mu and Beta frequency bands. Thereto, the preprocessed EEG data were
329 band-pass filtered in the 8 to 30 Hz frequency range. We then computed an
330 ICA to this filtered data. This procedure of applying an ICA decomposition to a
331 specific frequency-band is able to outperform the traditional wide-band ICA
332 both in terms of signal-to-noise ratio of the separated sources and in terms
333 of the number of the identified independent components ⁷². On the basis of
334 the ICs resulting from the ICA algorithm, equivalent current dipoles were
335 fitted using a four-shell spherical head model and standard electrode
336 positions (DIPFIT toolbox ^{73,74}). Then, to cluster ICs across participants, feature

337 vectors were created combining differences in spectra (8–30 Hz), dipole
 338 location, and scalp topography. Clusters were next identified using a k-means
 339 clustering algorithm ($k = 12$) in EEGLAB. Among the resulting clusters, a
 340 single sensorimotor cluster was visually identified in each experiment (i.e.,
 341 discrete and rhythmic) based on a centroparietal lateralized topography and
 342 a time-frequency map showing a clear ERD/ERS pattern.

343 In order to analyze the ERD/ERS activity of the MU and Beta bands,
 344 each IC of the two obtained clusters (i.e., discrete and rhythmic) was
 345 subjected to a time-frequency decomposition (using customized scripts
 346 written on Matlab) as follows: The EEG signals locked to the primary stimulus
 347 were convolved with complex 3-to-8 cycle-long Morlet's wavelets. Their
 348 central frequencies were changed from 8 to 30 Hz in 0.5 Hz steps (and from
 349 0.5 to 50 Hz for the C3 channel analysis in Appendix B). From the wavelet
 350 transformed signal, $w_k(t, f)$, of trial k at time t (3.5 ms time resolution) and
 351 with frequency f , the instantaneous power spectrum
 352 $p_k(t, f) = R(w_k(t, f))^2 + I(w_k(t, f))^2$ was extracted (R and I symbolize the real and
 353 imaginary parts of a complex number, respectively). The mean power
 354 spectrum (i.e., averaged across trials) was then computed for each
 355 participant in the GO_D, CONTINUE, STOP_D, STOP_R and GO_R conditions as follow:

$$356 \text{ Power} = \frac{1}{N} \cdot \sum_{k=1}^N p_k(t, f), (N = \text{number of trials}).$$

357 The power spectrum was then normalized with respect to a -400 to -100 ms
 358 pre-stimulus baseline and transformed to decibel scale ($10 \cdot \log_{10}$ of the sig-
 359 nal). In the rhythmic experiment, the baseline was extracted from the aver-
 360 aged GO_R trials (as in CONTINUE and STOP_R conditions, the pre-stimulus pe-
 361 riod includes movement). This mean power (time \times frequency \times power) was
 362 next averaged along the frequency dimension in an 8 Hz - 13 Hz window to
 363 compute the Mu power and a 15 Hz - 30 Hz window for the Beta power time
 364 series (time \times power).

365 To detect significant ERD and ERS, the resulting Mu and Beta power
 366 time series of each condition was compared against the mean value of the

367 power in the baseline time range (-400 to -100 ms). These comparisons were
368 performed based on a non-parametric permutation procedure (see below).
369 Thus, each time-period for which the power values were significantly below
370 the baseline level was indexed as an ERD. Each time-period subsequent to an
371 ERD and for which power did not significantly differ from the baseline level
372 was indexed as an ERS. Each time-period including power values that were
373 significantly above the baseline level was indexed as a power-rebound. To
374 compare Mu and Beta dynamics between conditions, power time series were
375 pairwise compared using the same non-parametric permutation procedure
376 (see below).

377 *Brain sources reconstruction*

378 To estimate the brain structures pertaining to the clustered ICs, a
379 brain-source reconstruction procedure was applied. For each clustered IC, the
380 inverse ICA weight projections onto the original EEG channels were exported
381 to the sLORETA (standardized low-resolution brain electromagnetic tomogra-
382 phy) data processing module ⁷⁵. sLORETA provides a unique solution to the in-
383 verse problem ⁷⁵⁻⁷⁷. For sLORETA, the intracerebral volume is partitioned into
384 6239 voxels with a 5 mm spatial resolution. Then, the standardized current
385 density at each voxel is calculated in a realistic head model ⁷⁸ based on the
386 MNI152 template.

387 ***Statistical analysis***

388 To compare LRP time series between conditions at the group level, the
389 LRPs were subjected to a nonparametric permutation procedure ⁷⁹. Specifi-
390 cally, the 15 participants' LRPs were pooled over the two compared condi-
391 tions (15 per condition). Two sets of 15 LRPs were then drawn randomly (un-
392 paired) from this pool, and the differential grand-average LRP was computed
393 between the two sets. This procedure was repeated 10 000 times, thus pro-
394 ducing a LRP distribution based on shuffled data under the null hypothesis.
395 For each time point, a p value was computed as the proportion of these
396 pseudo-differential LRPs that exceeded the observed participants' average
397 differential LRP. This p value indicates whether the observed power distribu-
398 tion for the two conditions diverged more than expected for random data (p

399 = .05 threshold). To correct for multiple comparisons, we analyzed the result-
400 ing distributions of p values to compute p thresholds corresponding to the
401 2.5th percentile of the smallest, and the 97.5th percentile of the largest p val-
402 ues distribution⁸⁰. The same procedure was applied to the averaged Mu and
403 Beta power time series to, first, assess ERD and ERS significance by compar-
404 ing power time series against baseline values and, second, to asses power
405 difference significance between conditions. [In the case of the Mu and Beta](#)
406 [power time series, the between-experiment comparison included an unequal](#)
407 [number of ICs \(20 discrete vs. 19 rhythmic ICs, respectively, see Results sec-](#)
408 [tion\). This variation was accounted for in the random-permutation stage of](#)
409 [the statistical procedure by randomly selecting a pool of 19 ICs from each ex-](#)
410 [perimentation at each iteration.](#)

411 Additionally, the study included measures of self-reported impulsivity,
412 which were correlated with the EEG measures. This exploratory analysis was
413 delegated to Appendix C for reasons of focus.

414 **Results**

415 ***Behavior***

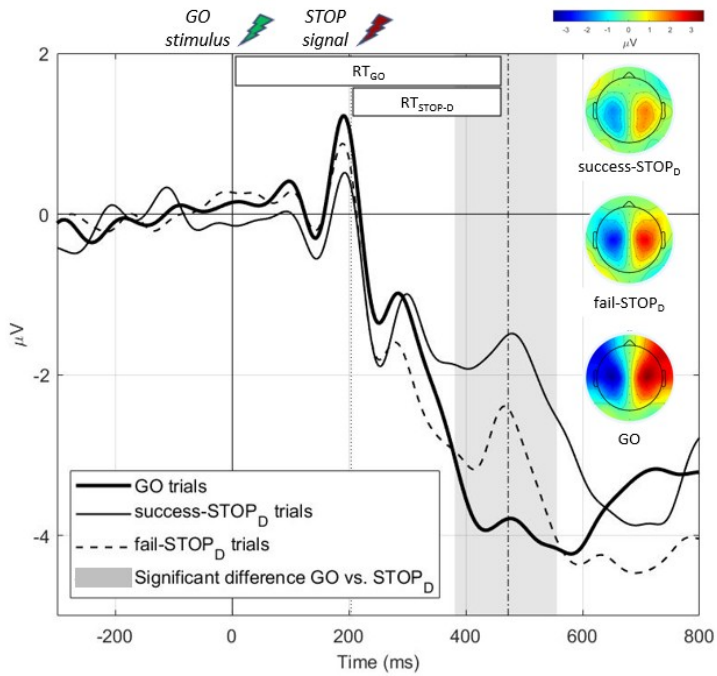
416 In the discrete experiment, the RT_{GO} ($M = 472$ ms, $SD = 64$ ms) and re-
417 sponse probability ($M = .54$, $SD = .08$) permitted the estimation of individ-
418 ual's RT_{STOP-D} ($M = 269$ ms, $SD = 45$ ms). The average STOP-signal delay
419 (SSD) for participants was 203 ms ($SD = 79$ ms). In the rhythmic experiment,
420 the spontaneous oscillation frequency was 1.65 Hz on average ($SD = 0.54$
421 Hz) and the analysis of the obtained StopTimes ($M = 399$, $SD = 34$ ms) en-
422 abled the computation of individual's RT_{STOP-R} ($M = 268$, $SD = 24$ ms). Impor-
423 tantly, the RT_{STOP-D} and the RT_{STOP-R} values did not differ ($t = .03$, $p > .05$) and
424 were unrelated across participants ($r = .02$, $p > .05$), suggesting independent
425 but comparable timing of inhibition processing between the two experiments.

426 ***Lateralized readiness potentials***

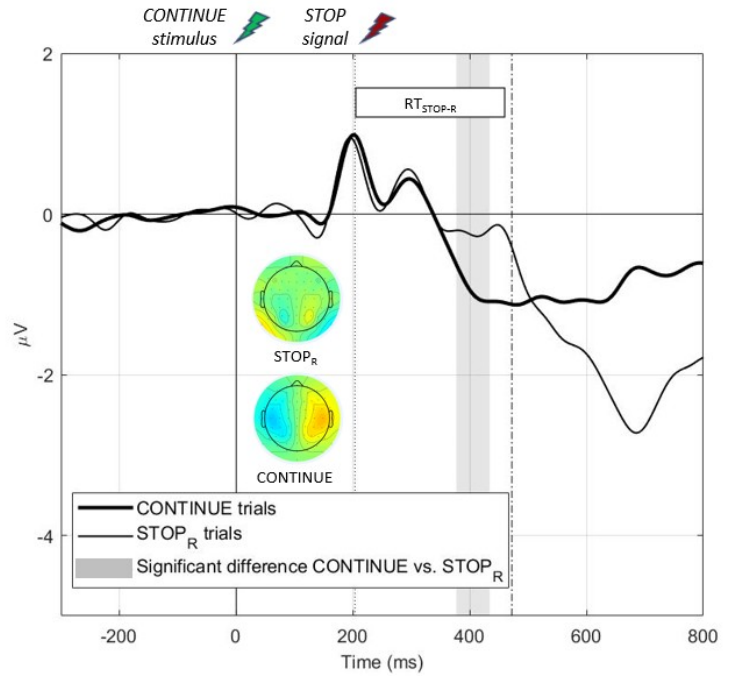
427 In every condition, the LRP computation resulted in a typical negative
428 deflection as portrayed in Fig. 1. In the discrete experiment, the permutation
429 analysis identified a significant difference in the 381 - 556 ms time window (p
430 $< .05$, corrected) between GO_D and successful- $STOP_D$ conditions (Fig. 1.A) and
431 in the 419 - 493 ms window between GO_D and fail- $STOP_D$ conditions. In the
432 rhythmic experiment, the same procedure identified a significant difference
433 in the 377 - 434 ms time window ($p < .05$, corrected) between CONTINUE and
434 $STOP_R$ conditions (Fig. 1.B). To compare the "inhibitory effect" between the
435 LRPs from the two experiments, differential LRPs were computed based on
436 the GO_D minus successful- $STOP_D$ difference for the discrete one and the CON-
437 TINUE minus $STOP_R$ difference for the rhythmic one. The two differential LRPs
438 were next compared through the same nonparametric permutation proce-
439 dure, which revealed that the LRP reduction was significantly larger in the
440 discrete experiment than in the rhythmic one in the 402 - 1,243 ms time win-
441 dow ($p < .05$, corrected; Fig. 1.C). Still, the peak amplitude of the differential
442 LRP was significantly correlated between discrete and rhythmic experiments
443 (*Pearson* $r = .96$, $p < .001$). Additionally, the exploratory analysis of individ-

444 ual's motor impulsivity indicated a significantly lower LRP peak amplitude for
445 the more impulsive participants in the GO_D and fail-STOP_D conditions (details
446 in Appendix C.).

A. Discrete experiment



B. Rhythmic experiment



C. Discrete vs. Rhythmic inhibitory effect

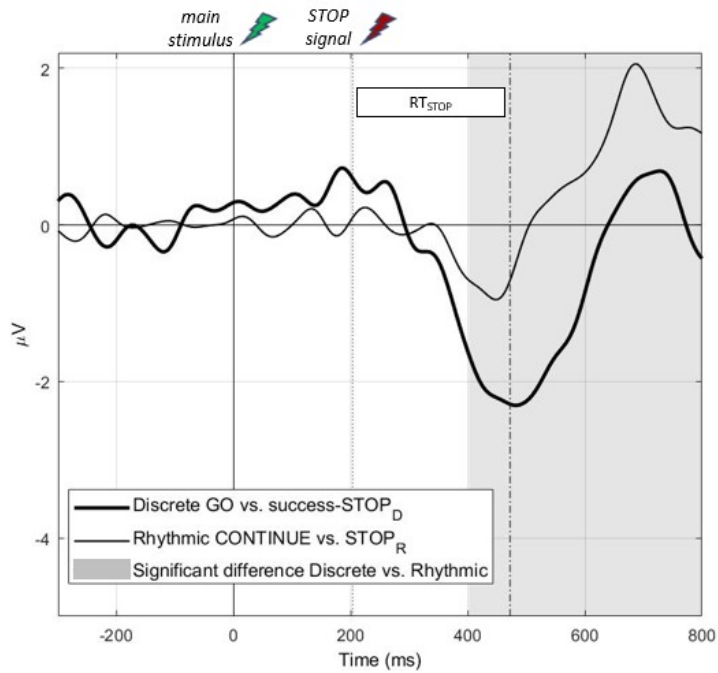


Fig.1: LRP analysis

Panel A: LRP (grand-average) computed in the discrete GO_D , success- $STOP_D$, and fail- $STOP_D$ conditions. GO_D LRP differed significantly from success- $STOP_D$ and fail- $STOP_D$ conditions. In grey, the region of significant difference (according to the nonparametric permutation analysis) between GO_D and success- $STOP_D$ conditions ($p < .05$, corrected).

Panel B: LRP (grand-average) computed in the rhythmic CONTINUE and $STOP_R$ conditions. In grey, the region of significant difference between the two conditions ($p < .05$, corrected).

Topographies are presented in panels A and B as the lateralized topographies computed at each condition LRP peak latency (see Method section).

Panel C: LRP inhibitory effect computed in the discrete (GO_D minus success- $STOP_D$ LRP) and the rhythmic (CONTINUE minus $STOP_R$ LRP) experiments. In grey, the region of significant difference between these two differential LRPs ($p < .05$, corrected).

The represented SSD, RT_{GO} and RT_{STOP} latencies are based on the average of the obtained latencies over all the participants. LRPs were 15 Hz low-pass filtered for graphical purpose.

449 ***Mu and Beta oscillations***

450 The power maps resulting from the time-frequency decomposition ap-
451 plied to the preprocessed EEG data of the C3 channel (0.5 to 50 Hz) are
452 shown for the different conditions in Appendix B.

453 In both experiments, only one sensorimotor cluster could be identified.
454 Thus, a single sensorimotor cluster of 20 ICs (contribution of 15 participants)
455 was retained for the discrete experiment. Another single cluster of 19 ICs was
456 retained (15 participants) for the rhythmic experiment (Fig. 2.A). The power
457 maps resulting from the time-frequency decomposition applied to the clus-
458 tered components (8 to 30 Hz) are shown in Fig. 2.B. The detailed time
459 course of Mu (8 - 13 Hz) and Beta (15 - 30 Hz) bands power and significant
460 ERD/ERS are highlighted in Fig. 3. Overall, Mu and Beta power show the ex-
461 pected dynamics, that is, an ERD during the movement execution. This ERD
462 appeared transient in the context of a discrete movement execution and sus-
463 tained when the movement was rhythmic. The Mu/Beta ERD were followed by
464 an ERS (Fig. 3). Notably, the ERS significantly exceeded the baseline level in
465 the STOP_R condition only, evidencing of a post-movement Mu and Beta re-
466 bound in this condition.

467 The Mu and Beta time-series were then compared between the experi-
468 mental conditions in a pairwise fashion (non-parametric permutation proce-
469 dure, see Method). The detailed result of these comparisons is provided in Ta-
470 ble 1. Importantly, Mu power did not vary significantly between the three con-
471 ditions of the discrete experiment: there was no significant difference the be-
472 tween movement-executed conditions (GO_D and fail-STOP_D) and the no-ac-
473 tual-movement condition (success-STOP_D). In the rhythmic experiment, the
474 significantly higher Mu power in the STOP_R condition characterized a post-
475 movement Mu ERS that was not present in the GO_R and CONTINUE conditions.
476 When comparing the two experiments, the Mu power increase was stronger
477 after the forced rhythmic-movement stop in the STOP_R condition as compared
478 to all the other conditions, including the GO_D and success-STOP_D conditions,
479 which are associated with a discrete-movement normal completion and can-
480 cellation, respectively.

481 Regarding the Beta power, the discrete conditions GO_D and fail-STOP_D
482 in which the movement was executed did not significantly differ. In contrast,
483 the success-STOP_D condition exposed a higher Beta power than GO_D, from
484 1,161 to 1,287 ms, and than fail-STOP_D, from 559 to 1,328 ms. In the rhythmic
485 experiment, the significantly higher Beta power in the STOP_R condition re-
486 lated to a post-movement Beta ERS that was not present in the GO_R and CON-
487 TINUE conditions (Fig. 3.). When comparing the two experiments, the pattern
488 of differences was similar to the Mu power, with the post-movement Beta
489 power increase being stronger in the STOP_R than the GO_D or the success-
490 STOP_D. Additionally, the exploratory analysis of individual's motor impulsivity
491 indicated significantly a higher PMBR amplitude for the more impulsive partic-
492 ipants in the STOP_R conditions (details in Appendix C.).

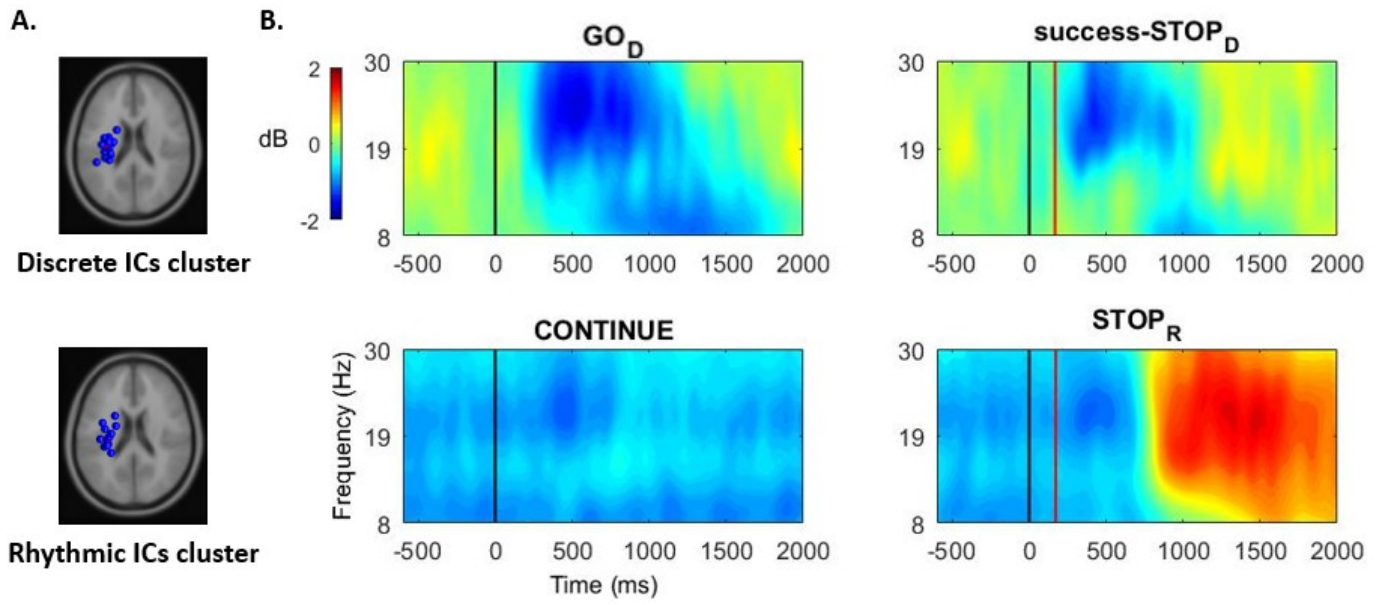
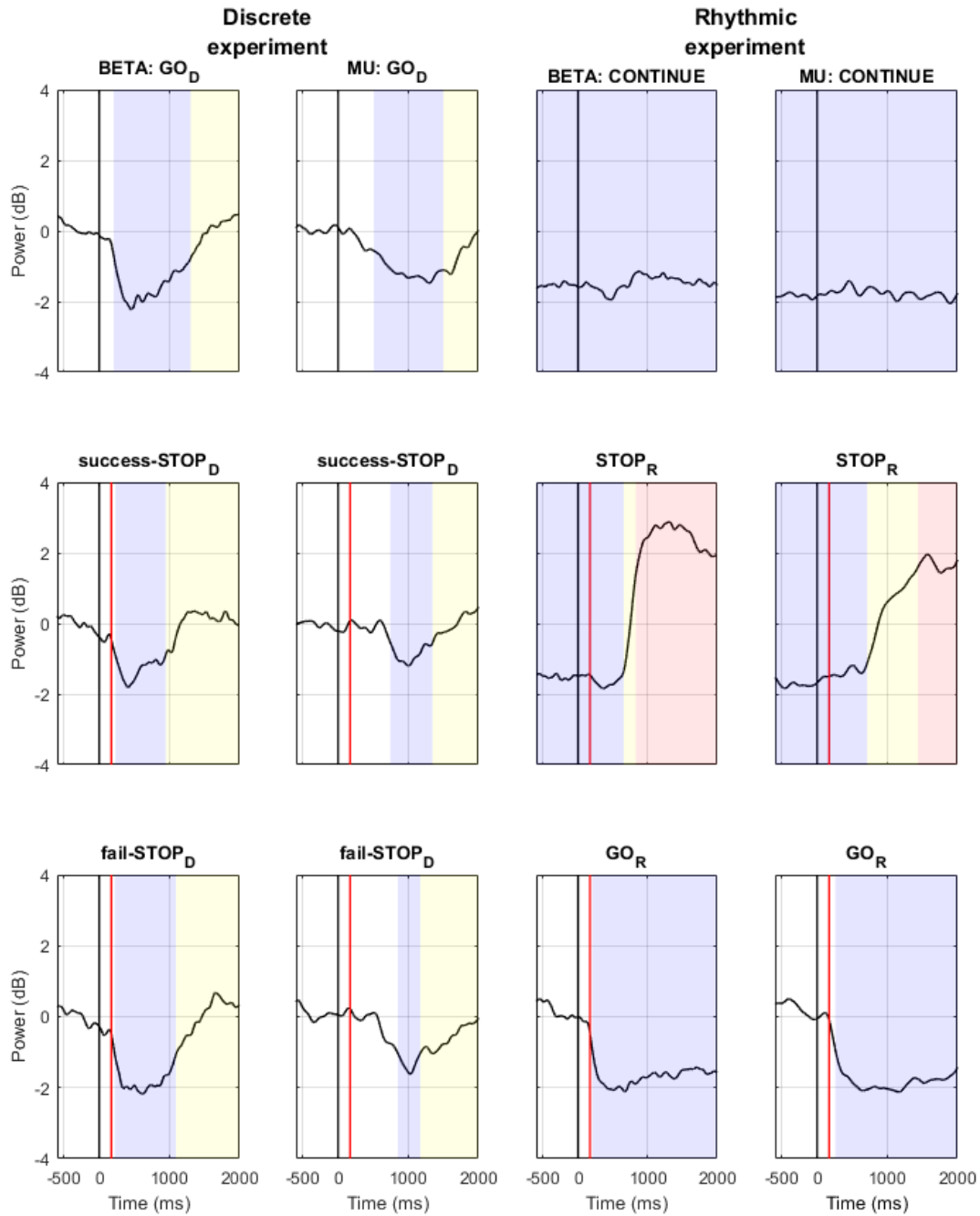


Fig.2: Component dimension time-frequency power analysis

Panel A: Equivalent current dipoles of the clustered sensorimotor components in the discrete (15 participants, 20 ICs) and the rhythmic (15 participants, 19 ICs) experiments.

Panel B: Time-frequency power maps (ICs grand-average) computed in the discrete (GO_D and $success-STOP_D$) and rhythmic ($CONTINUE$ and $STOP_R$) conditions. Black line: Primary (GO or $CONTINUE$) stimulus onset. Red line: $STOP$ signal onset (the represented onset is based on the average of the obtained SSD, over all the participants). The blue scale represents desynchronization and the red scale (re)synchronization of the brain activity.



495

Fig.3: Beta and Mu power time series

Power time series (ICs grand-average) averaged in the Beta (15 to 30 Hz) and the Mu (8 to 13 Hz) frequency ranges from the time-frequency power maps computed in the discrete (GO_D , $success-STOP_D$ and $fail-STOP_D$) and rhythmic ($CONTINUE$, $STOP_R$ and GO_R) conditions. Black line: Primary (GO or CONTINUE) stimulus onset. Red line: STOP signal onset (the represented onset is based on the average of the obtained SSD, over all the participants). Resulting from the non-parametric permutation comparison against baseline value, blue, yellow and red colors indicate time-ranges of significant ERD, ERS and power-rebound, respectively (see Method).

BETA power	GO _D	success-STOP _D	fail-STOP _D	CONTINUE	STOP _R	GO _R
MU power						
GO _D	-	Higher success-STOP _D power from 1,161 to 1,287 ms $z > 1.1473$	N.S. $z < 1.1911$	Higher GO _D power from -1,500 to 154 ms and from 1,468 to 2,000 ms $z > 1.2438$	Higher GO _D power from -1,500 to 172 ms and higher STOP _R power from 748 to 1,860 ms $z > 1.7282$	Higher GO _D power from 1,374 to 2,000 ms $z > 1.2392$
success-STOP _D	N.S. $z < 1.5210$	-	Higher success-STOP _D power from 559 to 1,328 ms $z > 1.1018$	Higher success-STOP _D power from -1,500 to 10 ms and from 1,133 to 2,000 ms $z > 1.1908$	Higher success-STOP _D power from -1,500 to 154 ms and higher STOP _R power from 780 to 2,000 ms $z > 1.5789$	Higher success-STOP _D power from 1,091 to 2,000 ms $z > 1.1954$
fail-STOP _D	N.S. $z < 1.4692$	N.S. $z < 1.4689$	-	Higher fail-STOP _D power from -1,500 to 179 ms and from 1,447 to 2,000 ms $z > 1.2893$	Higher fail-STOP _D power from -1,500 to 167 ms and higher STOP _R power from 741 to 1,654 ms $z > 1.7432$	Higher fail-STOP _D power from 1,325 to 2,000 ms $z > 1.2455$
CONTINUE	Higher GO _D power from -1,500 to 397 ms and from 1,871 to 2,000 ms $z > 1.6163$	Higher success-STOP _D power from -1,500 to 664 ms and from 1,458 to 2,000 ms $z > 1.6883$	Higher fail-STOP _D power from -1,500 to 399 ms and from 1,804 to 2,000 ms $z > 1.5852$	-	Higher STOP _R power from 773 to 2,000 ms $z > 1.7528$	Higher GO _R power from -1,500 to 164 ms $z > 1.1942$
STOP _R	Higher GO _D power from -1,500 to 331 ms and higher STOP _R power from 958 to 2,000 ms $z > 1.7832$	Higher success-STOP _D power from -1,500 to 189 ms and higher STOP _R power from 979 to 2,000 ms $z > 1.7575$	Higher fail-STOP _D power from -1,500 to 175 ms and higher STOP _R power from 928 to 2,000 ms $z > 1.7198$	Higher STOP _R power from 888 to 2,000 ms $z > 1.9067$	-	Higher GO _R power from -1,500 to -395 ms and higher STOP _R power from 755 to 2,000 ms $z > 1.8822$
GO _R	N.S. $z < 1.5813$	Higher success-STOP _D power from 493 to 2,000 ms	Higher fail-STOP _D power from 1,152 to 2,000 ms	Higher GO _R power from -1,500 to 178 ms $z > 1.6104$	Higher GO _R power from -1,500 to -216 ms and higher STOP _R power	-

		$z > 1.6655$	$z > 1.5310$		from 865 to 2,000 ms $z > 1.9595$	
--	--	--------------	--------------	--	---	--

496

497

Table 1: Pairwise condition comparison of Mu and Beta power time series

Mu and Beta power time series from the clustered ICs were compared between experimental conditions in a pairwise fashion using a non-parametric permutation procedure (see Method section). The resulting time-ranges of significant difference between conditions are reported.

Z values indicate the threshold values corresponding to $p < .05$ (corrected for multiple comparisons, see Method) retained to assess significance.

N.S. Non-significant.

498 **Brain sources reconstruction**

499 Based on the voxel-based sLORETA images, we searched for brain acti-
500 vation using voxel-wise randomization t -tests with 5000 permutations, based
501 on nonparametric statistical mapping. This procedure was performed sepa-
502 rately for the ICs of the discrete and rhythmic clusters. Significant voxels ($p <$
503 $.01$, corrected for multiple comparisons) were located in the MNI-brain (Fig. 4)
504 regarding the engaged Brodmann areas (BA) and the voxels coordinates. In
505 the discrete experiment, the clustered ICs activity was related to the activa-
506 tion of sensory regions such as the primary somatosensory (BA 1, BA 2, BA 3)
507 and the somatosensory association (BA 5) cortices, as well as M1 (BA 4). In
508 the rhythmic experiment, activation was found in the primary somatosensory
509 cortex (BA 3), as well as pre-motor areas (BA 6), and M1 (BA 4) (detailed MNI
510 coordinates of the activation are provided in Table 2).

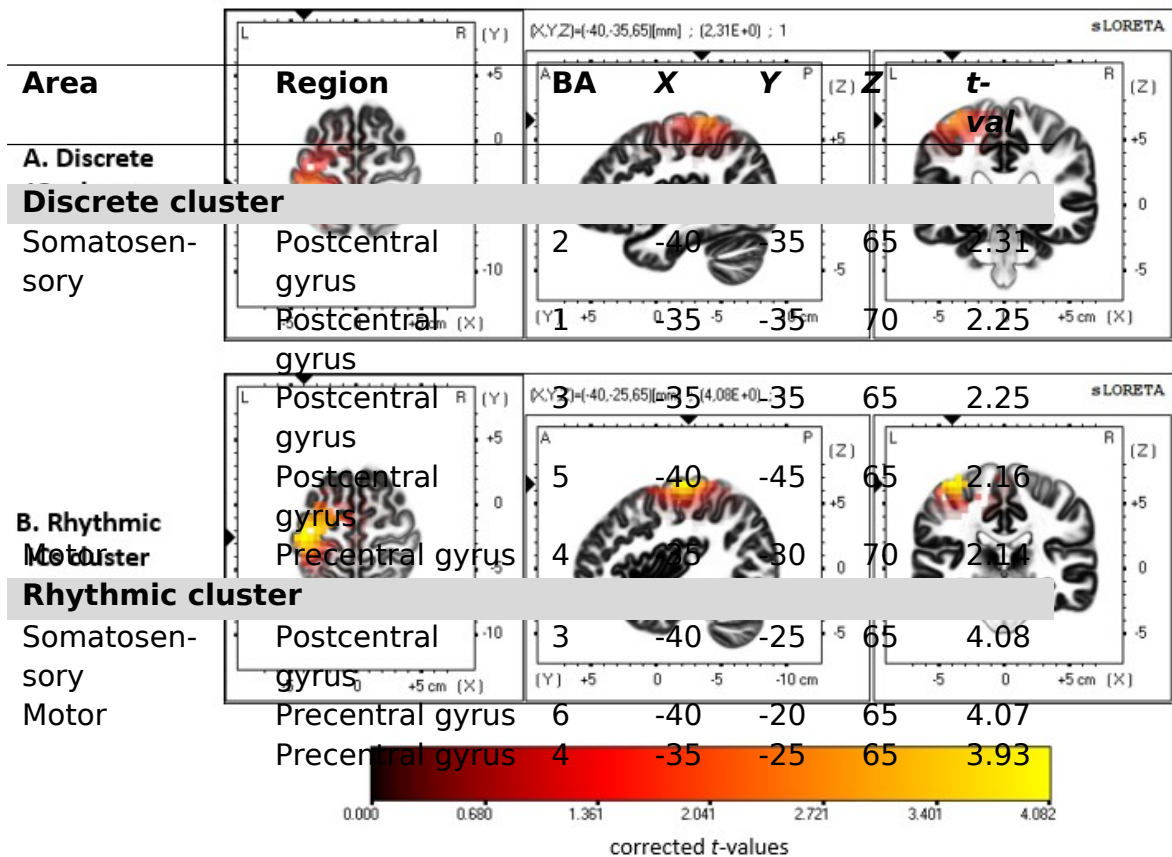


Fig.4: Brain sources reconstruction

The sLORETA images showing significant estimated activation pertaining to the discrete (**panel A**) and rhythmic (**panel B**) clustered ICs, for three orthogonal brain slices (horizontal, sagittal, coronal).

Only the voxels that passed the p value threshold ($p < .01$, corrected) are shown in color. The color represents t value. In the discrete experiment, activation was found in sensory (BA 1, BA 2, BA 3, BA 5) and motor areas (BA 4). In the rhythmic experiment, fewer sensory (BA 3) but (one) more motor regions (BA 4, BA 6) were involved. Detailed MNI localization of the significant activation is provided in Tab. 2.

511

513 **Discussion**

514 d to
 515 yth-
 516 ight
 517 and
 518 tical

519 ERD/ERS pattern identified over peri-Rolandic areas closely overlap those re-
 520 ported in previous work ^{14,50,52,62}. Indeed, we identified both somatosensory
 521 and motor cortical areas as generators of the observed ERD/ERS pattern, sup-
 522 porting the idea that both movement-related and sensory-related neural ac-
 523 tivity may be engaged. The inhibition mechanism triggered by the STOP sig-
 524 nal affected the LRP in both the discrete and rhythmic experiments, and oc-
 525 curred before the end of the RT_{GO} , RT_{STOP-D} , or RT_{STOP-R} latencies. Additionally,
 526 the measured RT_{GO} for movement generation and RT_{STOP} for movement sup-
 527 pression fell in the time range classically observed in stop-signal experiments
 528 across various movement responses ⁸¹⁻⁸⁴. The similarity between the discrete
 529 and the rhythmic RT_{STOP} values indicates that the processes engaged in abort-
 530 ing the two movement classes are of comparable duration.

531 Our first expectation dealt with the LRP dynamics. We hypothesized a
 532 large LRP following a GO stimulus to contrast with the absence of an LRP (i.e.,
 533 zero amplitude) following a CONTINUE stimulus, and that this LRP amplitude
 534 would be reduced by the STOP signal occurrence only in the discrete experi-
 535 ment. For the discrete movements, an LRP was triggered by the primary GO
 536 stimulus, and was subsequently impacted by the STOP signal in both success-
 537 ful- $STOP_D$ and failed- $STOP_D$ trials. These findings are consistent with the no-
 538 tion that an inhibition signal that arrives at M1 attenuates cortical motor out-
 539 flow, as reflected by the reduction of the LRP amplitude ⁴⁰; in the case of fail-
 540 $STOP_D$ trials, this reduction is insufficient to restraint the response threshold
 541 to be reached ³³. For the rhythmic movements, the CONTINUE stimuli occur-
 542 ring during the ongoing movement also led to an LRP response, albeit weaker
 543 than in the GO_D instruction. Rebutting our hypothesis, this LRP response indi-

544 cates that the presentation of the CONTINUE stimulus during the ongoing
545 movement triggers a non-negligible cortical motor activity. Thus, LRP might
546 not index pre-movement processing only, but also any cortical motor activity
547 occurring before and during movement. Alternatively, if the rhythmic move-
548 ment is implemented as a concatenation of discrete units, the LRP might re-
549 fect the cortical motor activity engaged in the initiation of each unit. Indeed,
550 previous studies have shown that the sensorimotor activity recorded in rhyth-
551 mic movements suggested a discrete-units-concatenation when the move-
552 ment frequency was ranging from 0.33 to 1 Hz, whereas this activity was
553 'truly' continuous for above 1 Hz movement frequencies^{31,32}. Nevertheless, as
554 the rhythmic movements in the present study were, on average, performed
555 at 1.65 Hz, the LRP observed in the CONTINUE trials are unlikely to reflect
556 motor cortical activity related to the concatenation of discrete movements.

557 The LRP amplitude following the CONTINUE stimulus was reduced in
558 the STOP_R condition. Notably, the amplitude of this "inhibitory effect", albeit
559 weaker, was strongly correlated to the GO minus STOP_D LRP difference mea-
560 sured in the discrete experiment. Thus, the LRP reduction might index action
561 inhibition in the context of both prepared-discrete and ongoing-rhythmic
562 movement suppression. This interpretation is consistent with the notion that
563 LRP is a marker of the cortical motor activity as a common final pathway in
564 the central control of movement and thus be the "site" where (frontal) execu-
565 tive "agents" exert inhibitory control⁸⁵. Note that the commonality of the mo-
566 tor site of inhibition in discrete and rhythmic action inhibition does not pro-
567 vide information about the inhibiting "agents" engaged in the two situations,
568 as the two levels of inhibition processing can be independent⁴⁰. Notably, the
569 EEG markers of the executive agents engaged in action inhibition tended to
570 dissociate the processing of discrete action cancelling and rhythmic action
571 stopping⁴³.

572 Our second expectation that the Mu ERD/ERS observed pattern should
573 show a transient vs. sustained activity for the discrete and rhythmic experi-
574 ments, respectively, was confirmed. This validates the discrete vs. rhythmic
575 nature of the performed movements and aligns with the understanding of the
576 Mu rhythm as a correlate of the interaction between sensory and motor infor-

577 mation processing: The sustained ERD during ongoing movement may corre-
578 spond to a closed-loop control for the online control of the ongoing move-
579 ment. In contrast, the transient Mu ERD/ERS pattern did not differ between
580 the performed discrete actions in the GO_D and fail-STOP_D conditions and the
581 cancelled ones in the success-STOP_D condition. This finding is in line with the
582 Mu rhythm being independent of the movement outcome, which may be the
583 case if the Mu rhythm encodes the processing of sensorimotor integration in
584 an open-loop control of discrete actions. Notably, the reactive inhibition of
585 discrete actions has been coherently conceptualized as a dual-step process
586 encompassing attention reorientation (by the STOP signal) and prepared-
587 movement cancellation⁸⁶⁻⁸⁸. The reorientation of attention is not specific to
588 action inhibition but generalizes to multiple situations implicating goal redi-
589 rection, including the reaction to a GO stimulus⁸⁸. Following the hypothesis
590 that the Mu rhythm is an alpha-like oscillation that links perception and action
591^{49,50}, a Mu ERD is expected to occur when cortical motor activity is modulated
592 following attentional reorientation, which includes both discrete GO_D and
593 STOP_D trials. Hence, the absence of actual movement in successful-STOP_D tri-
594 als should not modulate the Mu rhythm dynamics relative to Mu rhythm in
595 GO_D trials. Our results are in accordance with this expectation. A compatible
596 finding is that the Mu ERD/ERS varies with attention⁸⁹.

597 Confirming our third expectation, the Beta ERD appeared sustained for
598 the ongoing rhythmic movement whereas it was transient for the discrete
599 movement, thus following the motor activation dynamics. Next, a Beta ERS
600 occurred following the action. This is consistent with the purported role of the
601 Beta ERS in evaluating the action sensory output, in that it was lower for dis-
602 crete-movement failed cancellation compared to successful cancellation. Pre-
603 vious findings already reported this "error-related Beta rebound reduction",
604 which may relate to salient error/mismatch detection mechanisms^{90,91}. Still,
605 some results diverged from our expectations. On the one hand, the PMBR
606 was higher following a forced rhythmic movement stop (STOP_R) than the Beta
607 ERS following discrete movement completion (GO_D). On the other hand, the
608 discrete-action Beta ERS was higher after a successful action cancellation
609 than following action completion in GO_D and fail-STOP_D conditions, which did

610 not differ in this regard. These two findings support the notion that a higher
611 Beta ERS is a correlate of active action suppression¹⁴, here triggered by a
612 STOP signal. Whereas Parkes et al. identified PMBR neural generators in post-
613 Rolandic (sensory) areas, which they interpreted in favor of the notion that
614 PMBR reflects sensory reafference evaluation⁵⁹, other studies suggested that
615 the PMBR was also related to pre-Rolandic (motor) activation^{58,92,93}. Our re-
616 sults are in line with the latter findings, with both a significant PMBR and pre-
617 motor activation being reported for the rhythmic but not discrete actions.
618 This engagement of pre-motor cortices in the rhythmic movements is congru-
619 ent with the previously reported pre-supplementary motor area activation in
620 PMBR^{94,95}. Thus, our results do not exclude that Beta ERS is an index of ac-
621 tion sensory outcome evaluation, but they also support the view that it is as-
622 sociated with an active inhibition process of cortical motor activity.

623 Nonetheless, this active inhibition hypothesis of the PMBR functional
624 role is silent on why the ongoing action-forced stop gave rise to a large PMBR
625 over contralateral sensorimotor cortical areas, whereas a much weaker Beta
626 ERS followed discrete action cancellation. A tentative explanation is that the
627 inhibitory process engaged in movement cancellation acts at the movement
628 preparation level, as indicated by the LRP decrease and the ERD abortion in
629 the STOP_D condition⁴¹. Thus, inhibition might lie in maintaining the cortical
630 idle state to cancel a discrete action, whereas it would force the return to this
631 idle state to stop a rhythmic movement. This explanation is also consistent
632 with the notion that a discrete action, if controlled in an open-loop fashion, is
633 not associated with an online control based on sensory prediction evaluation,
634 as the PMBR is a correlate of the latter. In contrast, if controlled in a closed-
635 loop fashion, the ongoing-rhythmic action requires the evaluation of the sen-
636 sory predictions associated with the movement production, as indicated by a
637 significant PMBR. A distinction in the movement-suppression after-effect (i.e.,
638 PMBR) suggests that discrete-action cancelling and rhythmic-action stopping
639 may engage distinct inhibition processes⁴³. As action inhibition operates on
640 both discrete^{64,81} and rhythmic^{4-6,42} movements, considering the distinction
641 between the two movement classes would undoubtedly contribute to a better
642 understanding of this complex process at the neurobiological level.

643 Alternatively, the lower Beta ERS following discrete action completion
644 and cancellation compared to the large PMBR following rhythmic action stop,
645 may reflect a PMBR that has been reduced due to the task uncertainty. In-
646 deed, previous work suggested that beta power reflects the estimated uncer-
647 tainty in the parameters of the forward models involved in motor control ⁹⁶.
648 Thus, the primary stimuli (blue or green) in the discrete experiment required
649 a two-choice reaction (i.e., trigger a discrete movement toward the left or
650 right side), whereas the same stimuli required a unique response in the
651 rhythmic experiment (i.e., continue the movement for both blue and green
652 stimuli). This discrepancy may introduce a modulation of confidence in the
653 predicted sensory outcome in the forward model of action control, resulting in
654 a lower post-movement Beta modulation ^{54,96}. In contrast, the rhythmicity of
655 an ongoing movement may lead to a confident movement execution that in-
656 creases the PMBR ⁹⁷.

657 Overall, our pattern of results regarding the Beta power dynamics ex-
658 cludes an understanding of the PMBR neither as a correlate of the action sen-
659 sory outcome evaluation nor as an index of active motor suppression. In fact,
660 both interpretations are not incompatible, and a tentative explanation is that
661 the PMBR reflects the action control in forward models, with its amplitude be-
662 ing modulated by the uncertainty and the engagement of an inhibition
663 process. Thus, the PMBR could be reduced when the uncertainty of the pre-
664 dicted sensory output is high, whereas it would be strengthened in reaction
665 to an inhibition signal. This imperative action suppression might result in sup-
666 pressing the motor plan execution and its predicted sensory outcome. It
667 could also lead to the interruption of the closed-loop processing of sensorimo-
668 tor information itself, as indicated by the Mu rebound that followed the rhyth-
669 mic action stop. Although this explanation remains highly hypothetical with-
670 out studies manipulating sensory feedback and inhibition requirement, it
671 globally fits well with a recently established framework in which Beta re-
672 bounds reflect, at various cortical sites, a "clearing-out" of the motor plan ~~and~~
673 ~~the working memory~~⁹⁸.

674 The present study focused on the movement performance and sup-
675 pression in reaction to an external cue, so-called exogenous action control ⁹⁹.

676 Adapted behavior also includes performing and suppressing movement in a
677 self-initiated fashion, that is, endogenous motor control. Generalizing the
678 present functional interpretation of neural sensorimotor activities requires
679 that future experiments study and contrast both situations. Especially, inter-
680 nal and external movement initiation require partially distinct sensorimotor
681 activities ¹⁰⁰. Movement suppression mechanisms are also known to vary as a
682 function of whether proactive vs. reactive inhibition is required, both for the
683 suppression of discrete ^{101,102} and rhythmic ⁶ movements. These investigations
684 are much needed to provide a complete comprehension of sensorimotor cor-
685 tical activity.

686 The understanding of sensorimotor activity has implications for multi-
687 ple clinical syndromes associated with movement disorders ¹⁰³. The abilities
688 to initiate and stop action are especially affected by impulsivity ³, which is an
689 essential dimension of several psychiatric disorders, such as attention deficit
690 hyperactivity disorder (ADHD) and obsessive-compulsive disorder (OCD).
691 Evaluating neural sensorimotor activity through movement-related cortical
692 ERD/ERS, healthy participants have been distinguished from those with ADHD
693 ¹⁰⁴ and OCD ¹⁰⁵. In the general population, sensorimotor activity is poorly in-
694 vestigated in relation to individuals' impulsivity traits. A recent study sug-
695 gested that sensorimotor ERD/ERS amplitude may relate to impulsivity ¹⁰⁶.
696 The association reported in Appendix C. between motor impulsivity and lower
697 LRP amplitude in triggering a discrete action and higher PMBR when forced-
698 stopping a rhythmic action suggests that cortical sensorimotor activity in the
699 execution and suppression of action might depend on the individual's impul-
700 sivity level. Still, further studies targeting the impulsivity dimension and in-
701 cluding participants exhibiting a broad range of impulsivity levels are re-
702 quired to test this hypothesis.

703 Finally, the present study provides new insights in understanding the
704 cerebral sensorimotor activity by exploring EEG records of LRP and Mu/Beta
705 rhythms associated with the performance and suppression of movement in
706 the context of discrete and rhythmic classes of actions. Showing the distinct
707 sensorimotor dynamics that operate in the two action classes, our findings
708 are highly compatible with recent proposals that Mu and Beta rhythms might

709 encode reciprocal interactions between motor and sensory cortices to enable
710 movement monitoring ^{47,96}. Still, the PMBR may also reflect the engagement
711 of a clearing-out function to abort the sensorimotor processing when action
712 has to be inhibited ¹⁴. At any rate, our findings support the notion that Mu and
713 Beta frequency bands play complementary roles in the sensorimotor control
714 of action ~~and also converge with previous work showing that PMBR arises~~
715 ~~from a distributed network rather than a discrete cortical focus~~ ^{52,107}. Further
716 studies using imaging procedures with a better spatial resolution are required
717 to disentangle the Mu and Beta specific implication in the different cortical ar-
718 eas that engage in action performance and suppression.

719 **Data Availability**

720 The data generated during and/or analyzed during the current study are
721 available from the corresponding author upon reasonable request.

722 **References**

- 723 1. Riehle, A. & Vaadia, E. *Motor Cortex in Voluntary Movements: A*
724 *Distributed System for Distributed Functions*. (CRC Press, 2004).
- 725 2. Hogan, N. & Sternad, D. On rhythmic and discrete movements:
726 reflections, definitions and implications for motor control. *Exp. Brain*
727 *Res.* **181**, 13–30 (2007).
- 728 3. Bari, A. & Robbins, T. W. Inhibition and impulsivity: behavioral and
729 neural basis of response control. *Prog. Neurobiol.* **108**, 44–79 (2013).
- 730 4. Hervault, M., Huys, R., Farrer, C., Buisson, J. C. & Zanone, P. G.
731 Cancelling discrete and stopping ongoing rhythmic movements: Do
732 they involve the same process of motor inhibition? *Hum. Mov. Sci.* **64**,
733 296–306 (2019).
- 734 5. Lofredi, R. *et al.* Subthalamic stimulation impairs stopping of ongoing
735 movements. *Brain* **144**, 44–52 (2021).
- 736 6. Schultz, K. E., Denning, D., Hufnagel, V. & Swann, N. Stopping a
737 Continuous Movement: A Novel Approach to Investigating Motor
738 Control. *bioRxiv* 2021.04.08.439070 (2021)
739 doi:10.1101/2021.04.08.439070.
- 740 7. Sosnik, R., Chaim, E. & Flash, T. Stopping is not an option: the
741 evolution of unstoppable motion elements (primitives). *J. Neurophysiol.*
742 **114**, 846–856 (2015).
- 743 8. Alegre, M. *et al.* Frontal and central oscillatory changes related to
744 different aspects of the motor process: a study in go/no-go paradigms.
745 *Exp. Brain Res.* **159**, 14–22 (2004).

- 746 9. Leocani, L., Toro, C., Zhuang, P., Gerloff, C. & Hallett, M. Event-related
747 desynchronization in reaction time paradigms: a comparison with
748 event-related potentials and corticospinal excitability. *Clin.*
749 *Neurophysiol. Off. J. Int. Fed. Clin. Neurophysiol.* **112**, 923–930 (2001).
- 750 10. Savostyanov, A. N. *et al.* EEG-correlates of trait anxiety in the stop-
751 signal paradigm. *Neurosci. Lett.* **449**, 112–116 (2009).
- 752 11. Solis-Escalante, T., Müller-Putz, G. R., Pfurtscheller, G. & Neuper, C.
753 Cue-induced beta rebound during withholding of overt and covert foot
754 movement. *Clin. Neurophysiol. Off. J. Int. Fed. Clin. Neurophysiol.* **123**,
755 1182–1190 (2012).
- 756 12. Alegre, M., Alvarez-Gerriko, I., Valencia, M., Iriarte, J. & Artieda, J.
757 Oscillatory changes related to the forced termination of a movement.
758 *Clin. Neurophysiol.* **119**, 290–300 (2008).
- 759 13. Alegre, M. *et al.* Alpha and beta oscillatory activity during a sequence
760 of two movements. *Clin. Neurophysiol. Off. J. Int. Fed. Clin.*
761 *Neurophysiol.* **115**, 124–130 (2004).
- 762 14. Heinrichs-Graham, E., Kurz, M. J., Gehringer, J. E. & Wilson, T. W. The
763 functional role of post-movement beta oscillations in motor
764 termination. *Brain Struct. Funct.* **222**, 3075–3086 (2017).
- 765 15. Pakenham, D. O. *et al.* Post-stimulus beta responses are modulated by
766 task duration. *NeuroImage* **206**, 116288 (2020).
- 767 16. Guiard, Y. Fitts' law in the discrete vs. cyclical paradigm. *Hum. Mov.*
768 *Sci.* **16**, 97–131 (1997).

- 769 17. Huys, R., Studenka, B. E., Rheaume, N. L., Zelaznik, H. N. & Jirsa, V. K.
770 Distinct Timing Mechanisms Produce Discrete and Continuous
771 Movements. *PLoS Comput. Biol.* **4**, e1000061 (2008).
- 772 18. Huys, R., Studenka, B. E., Zelaznik, H. N. & Jirsa, V. K. Distinct timing
773 mechanisms are implicated in distinct circle drawing tasks. *Neurosci.*
774 *Lett.* **472**, 24–28 (2010).
- 775 19. Schaal, S., Sternad, D., Osu, R. & Kawato, M. Rhythmic arm movement
776 is not discrete. *Nat. Neurosci.* **7**, 1136–1143 (2004).
- 777 20. Spencer, R. M. C., Zelaznik, H. N., Diedrichsen, J. & Ivry, R. B. Disrupted
778 timing of discontinuous but not continuous movements by cerebellar
779 lesions. *Science* **300**, 1437–1439 (2003).
- 780 21. Wiegel, P., Kurz, A. & Leukel, C. Evidence that distinct human primary
781 motor cortex circuits control discrete and rhythmic movements. *J.*
782 *Physiol.* **598**, 1235–1251 (2020).
- 783 22. Zelaznik, H. N. & Lantero, D. The role of vision in repetitive circle
784 drawing. *Acta Psychol. (Amst.)* **92**, 105–118 (1996).
- 785 23. Jeannerod, M. *The neural and behavioural organization of goal-directed*
786 *movements*. xii, 283 (Clarendon Press/Oxford University Press, 1988).
- 787 24. Coles, M. G. H. Modern Mind-Brain Reading: Psychophysiology,
788 Physiology, and Cognition. *Psychophysiology* **26**, 251–269 (1989).
- 789 25. Pfurtscheller, G. & Lopes da Silva, F. H. Event-related EEG/MEG
790 synchronization and desynchronization: basic principles. *Clin.*
791 *Neurophysiol.* **110**, 1842–1857 (1999).

- 792 26. Alegre, M. *et al.* Alpha and beta oscillatory changes during stimulus-
793 induced movement paradigms: effect of stimulus predictability.
794 *Neuroreport* **14**, 381–385 (2003).
- 795 27. Gaetz, W., Macdonald, M., Cheyne, D. & Snead, O. C. Neuromagnetic
796 imaging of movement-related cortical oscillations in children and
797 adults: age predicts post-movement beta rebound. *NeuroImage* **51**,
798 792–807 (2010).
- 799 28. McFarland, D. J., Miner, L. A., Vaughan, T. M. & Wolpaw, J. R. Mu and
800 Beta Rhythm Topographies During Motor Imagery and Actual
801 Movements. *Brain Topogr.* **12**, 177–186 (2000).
- 802 29. Erbil, N. & Ungan, P. Changes in the alpha and beta amplitudes of the
803 central EEG during the onset, continuation, and offset of long-duration
804 repetitive hand movements. *Brain Res.* **1169**, 44–56 (2007).
- 805 30. Seeber, M., Scherer, R. & Müller-Putz, G. R. EEG Oscillations Are
806 Modulated in Different Behavior-Related Networks during Rhythmic
807 Finger Movements. *J. Neurosci.* **36**, 11671–11681 (2016).
- 808 31. Hermes, D. *et al.* Dissociation between Neuronal Activity in
809 Sensorimotor Cortex and Hand Movement Revealed as a Function of
810 Movement Rate. *J. Neurosci.* **32**, 9736–9744 (2012).
- 811 32. Toma, K. *et al.* Movement Rate Effect on Activation and Functional
812 Coupling of Motor Cortical Areas. *J. Neurophysiol.* **88**, 3377–3385
813 (2002).
- 814 33. De Jong, R., Coles, M. G. H., Logan, G. D. & Gratton, G. In search of the
815 point of no return: the control of response processes. *J. Exp. Psychol.*
816 *Hum. Percept. Perform.* **16**, 164–182 (1990).

- 817 34. de Jong, R., Gladwin, T. E. & 't Hart, B. M. Movement-related EEG
818 indices of preparation in task switching and motor control. *Brain Res.*
819 **1105**, 73–82 (2006).
- 820 35. Smulders, F. T. Y. & Miller, J. O. *The Lateralized Readiness Potential.*
821 (Oxford University Press, 2011).
822 doi:10.1093/oxfordhb/9780195374148.013.0115.
- 823 36. Gratton, G., Coles, M. G., Sirevaag, E. J., Eriksen, C. W. & Donchin, E.
824 Pre- and poststimulus activation of response channels: a
825 psychophysiological analysis. *J. Exp. Psychol. Hum. Percept. Perform.*
826 **14**, 331–344 (1988).
- 827 37. van Vugt, M. K., Simen, P., Nystrom, L., Holmes, P. & Cohen, J. D.
828 Lateralized Readiness Potentials Reveal Properties of a Neural
829 Mechanism for Implementing a Decision Threshold. *PLoS ONE* **9**,
830 (2014).
- 831 38. De Jong, R., Coles, M. G. H. & Logan, G. D. Strategies and mechanisms
832 in nonselective and selective inhibitory motor control. *J. Exp. Psychol.*
833 *Hum. Percept. Perform.* **21**, 498–511 (1995).
- 834 39. Galdo-Alvarez, S., Bonilla, F. M., González-Villar, A. J. & Carrillo-de-la-
835 Peña, M. T. Functional Equivalence of Imagined vs. Real Performance of
836 an Inhibitory Task: An EEG/ERP Study. *Front. Hum. Neurosci.* **10**,
837 (2016).
- 838 40. van Boxtel, G. J. M., van der Molen, M. W., Jennings, J. R. & Brunia, C. H.
839 M. A psychophysiological analysis of inhibitory motor control in the
840 stop-signal paradigm. *Biol. Psychol.* **58**, 229–262 (2001).

- 841 41. Wessel, J. R. Prepotent motor activity and inhibitory control demands in
842 different variants of the go/no-go paradigm. *Psychophysiology* **55**,
843 e12871 (2018).
- 844 42. Morein-Zamir, S., Chua, R., Franks, I., Nagelkerke, P. & Kingstone, A.
845 Measuring online volitional response control with a continuous tracking
846 task. *Behav. Res. Methods* **38**, 638–647 (2006).
- 847 43. Hervault, M., Zanone, P.-G., Buisson, J.-C. & Huys, R. Hold your horses:
848 Differences in EEG correlates of inhibition in cancelling and stopping an
849 action. (2021) doi:10.31234/osf.io/ys9pd.
- 850 44. Neuper, C., Wörtz, M. & Pfurtscheller, G. ERD/ERS patterns reflecting
851 sensorimotor activation and deactivation. in *Progress in Brain Research*
852 vol. 159 211–222 (Elsevier, 2006).
- 853 45. Pfurtscheller, G., Stancák, A. & Neuper, Ch. Event-related
854 synchronization (ERS) in the alpha band — an electrophysiological
855 correlate of cortical idling: A review. *Int. J. Psychophysiol.* **24**, 39–46
856 (1996).
- 857 46. Engel, A. K. & Fries, P. Beta-band oscillations—signalling the status
858 quo? *Curr. Opin. Neurobiol.* **20**, 156–165 (2010).
- 859 47. Saltuklaroglu, T. *et al.* EEG mu rhythms: Rich sources of sensorimotor
860 information in speech processing. *Brain Lang.* **187**, 41–61 (2018).
- 861 48. Wolpert, D. M., Ghahramani, Z. & Jordan, M. I. An internal model for
862 sensorimotor integration. *Science* **269**, 1880–1882 (1995).
- 863 49. Pineda, J. A. The functional significance of mu rhythms: Translating
864 “seeing” and “hearing” into “doing”. *Brain Res. Rev.* **50**, 57–68 (2005).

- 865 50. Hari, R. Action-perception connection and the cortical mu rhythm.
866 *Prog. Brain Res.* **159**, 253–260 (2006).
- 867 51. Sebastiani, V. *et al.* Being an agent or an observer: Different spectral
868 dynamics revealed by MEG. *NeuroImage* **102**, 717–728 (2014).
- 869 52. Kilavik, B. E., Zaepffel, M., Brovelli, A., MacKay, W. A. & Riehle, A. The
870 ups and downs of beta oscillations in sensorimotor cortex. *Exp. Neurol.*
871 **245**, 15–26 (2013).
- 872 53. Torrecillos, F., Alayrangues, J., Kilavik, B. E. & Malfait, N. Distinct
873 Modulations in Sensorimotor Postmovement and Foreperiod β -Band
874 Activities Related to Error Salience Processing and Sensorimotor
875 Adaptation. *J. Neurosci. Off. J. Soc. Neurosci.* **35**, 12753–12765 (2015).
- 876 54. Tzagarakis, C., Ince, N. F., Leuthold, A. C. & Pellizzer, G. Beta-band
877 activity during motor planning reflects response uncertainty. *J.*
878 *Neurosci. Off. J. Soc. Neurosci.* **30**, 11270–11277 (2010).
- 879 55. Cassim, F. *et al.* Does post-movement beta synchronization reflect an
880 idling motor cortex? *Neuroreport* **12**, 3859–3863 (2001).
- 881 56. Alegre, M. *et al.* Beta electroencephalograph changes during passive
882 movements: sensory afferences contribute to beta event-related
883 desynchronization in humans. *Neurosci. Lett.* **331**, 29–32 (2002).
- 884 57. Houdayer, E., Labyt, E., Cassim, F., Bourriez, J. L. & Derambure, P.
885 Relationship between event-related beta synchronization and afferent
886 inputs: analysis of finger movement and peripheral nerve stimulations.
887 *Clin. Neurophysiol. Off. J. Int. Fed. Clin. Neurophysiol.* **117**, 628–636
888 (2006).

- 889 58. Salmelin, R., Hämäläinen, M., Kajola, M. & Hari, R. Functional
890 segregation of movement-related rhythmic activity in the human brain.
891 *NeuroImage* **2**, 237-243 (1995).
- 892 59. Parkes, L. M., Bastiaansen, M. C. M. & Norris, D. G. Combining EEG and
893 fMRI to investigate the post-movement beta rebound. *NeuroImage* **29**,
894 685-696 (2006).
- 895 60. Elie, D., Desmyttere, G., Mathieu, E., Tallet, J. & Cremoux, S. Magnitude
896 of the post-movement beta synchronization correlates with the
897 variability of the ankle torque production. *Neurophysiol. Clin.* **48**, 226-
898 227 (2018).
- 899 61. Fry, A. *et al.* Modulation of post-movement beta rebound by
900 contraction force and rate of force development. *Hum. Brain Mapp.* **37**,
901 2493-2511 (2016).
- 902 62. Cheyne, D. O. MEG studies of sensorimotor rhythms: A review. *Exp.*
903 *Neurol.* **245**, 27-39 (2013).
- 904 63. Oldfield, R. C. The assessment and analysis of handedness: The
905 Edinburgh inventory. *Neuropsychologia* **9**, 97-113 (1971).
- 906 64. Verbruggen, F. *et al.* A consensus guide to capturing the ability to
907 inhibit actions and impulsive behaviors in the stop-signal task. *eLife* **8**,
908 e46323 (2019).
- 909 65. Trans Cranial Technologies. 10/20 System Positioning Manual. (2012).
- 910 66. Delorme, A. & Makeig, S. EEGLAB: an open source toolbox for analysis
911 of single-trial EEG dynamics including independent component
912 analysis. *J. Neurosci. Methods* **134**, 9-21 (2004).

- 913 67. Bell, A. J. & Sejnowski, T. J. An information-maximization approach to
914 blind separation and blind deconvolution. *Neural Comput.* **7**, 1129-
915 1159 (1995).
- 916 68. Pion-Tonachini, L., Kreutz-Delgado, K. & Makeig, S. ICLabel: An
917 automated electroencephalographic independent component classifier,
918 dataset, and website. *NeuroImage* **198**, 181-197 (2019).
- 919 69. Verbruggen, F. & Logan, G. D. Models of response inhibition in the
920 stop-signal and stop-change paradigms. *Neurosci. Biobehav. Rev.* **33**,
921 647-661 (2009).
- 922 70. Neuper, C. & Pfurtscheller, G. Event-related dynamics of cortical
923 rhythms: frequency-specific features and functional correlates. *Int. J.*
924 *Psychophysiol. Off. J. Int. Organ. Psychophysiol.* **43**, 41-58 (2001).
- 925 71. Zaepffel, M., Trachel, R., Kilavik, B. E. & Brochier, T. Modulations of EEG
926 Beta Power during Planning and Execution of Grasping Movements.
927 *PLOS ONE* **8**, e60060 (2013).
- 928 72. Jonmohamadi, Y. & Muthukumaraswamy, S. D. Multi-band component
929 analysis for EEG artifact removal and source reconstruction with
930 application to gamma-band activity. *Biomed. Phys. Eng. Express* **4**,
931 035007 (2018).
- 932 73. Delorme, A., Palmer, J., Onton, J., Oostenveld, R. & Makeig, S.
933 Independent EEG Sources Are Dipolar. *PLOS ONE* **7**, e30135 (2012).
- 934 74. Oostenveld, R. & Oostendorp, T. F. Validating the boundary element
935 method for forward and inverse EEG computations in the presence of a
936 hole in the skull. *Hum. Brain Mapp.* **17**, 179-192 (2002).

- 937 75. Pascual-Marqui, R. D. Standardized low-resolution brain
938 electromagnetic tomography (sLORETA): technical details. *Methods*
939 *Find. Exp. Clin. Pharmacol.* **24 Suppl D**, 5–12 (2002).
- 940 76. Marco-Pallarés, J., Grau, C. & Ruffini, G. Combined ICA-LORETA analysis
941 of mismatch negativity. *NeuroImage* **25**, 471–477 (2005).
- 942 77. Sekihara, K., Sahani, M. & Nagarajan, S. S. Localization bias and spatial
943 resolution of adaptive and non-adaptive spatial filters for MEG source
944 reconstruction. *NeuroImage* **25**, 1056–1067 (2005).
- 945 78. Fuchs, M., Kastner, J., Wagner, M., Hawes, S. & Ebersole, J. S. A
946 standardized boundary element method volume conductor model. *Clin.*
947 *Neurophysiol. Off. J. Int. Fed. Clin. Neurophysiol.* **113**, 702–712 (2002).
- 948 79. Maris, E. & Oostenveld, R. Nonparametric statistical testing of EEG- and
949 MEG-data. *J. Neurosci. Methods* **164**, 177–190 (2007).
- 950 80. Cohen, M. X. *Analyzing Neural Time Series Data – Theory and Practice.*
951 (MIT Press, 2014).
- 952 81. Boucher, L., Stuphorn, V., Logan, G. D., Schall, J. D. & Palmeri, T. J.
953 Stopping eye and hand movements: Are the processes independent?
954 *Percept. Psychophys.* **69**, 785–801 (2007).
- 955 82. Kok, A., Ramautar, J. R., De Ruiter, M. B., Band, G. P. H. & Ridderinkhof,
956 K. R. ERP components associated with successful and unsuccessful
957 stopping in a stop-signal task. *Psychophysiology* **41**, 9–20 (2004).
- 958 83. Krämer, U. M., Knight, R. T. & Münte, T. F. Electrophysiological
959 evidence for different inhibitory mechanisms when stopping or
960 changing a planned response. *J. Cogn. Neurosci.* **23**, 2481–2493
961 (2011).

- 962 84. Montanari, R., Giamundo, M., Brunamonti, E., Ferraina, S. & Pani, P.
963 Visual salience of the stop-signal affects movement suppression
964 process. *Exp. Brain Res.* **235**, 2203–2214 (2017).
- 965 85. Band, G. P. & van Boxtel, G. J. Inhibitory motor control in stop
966 paradigms: review and reinterpretation of neural mechanisms. *Acta*
967 *Psychol. (Amst.)* **101**, 179–211 (1999).
- 968 86. Wessel, J. R. & Aron, A. R. On the Globality of Motor Suppression:
969 Unexpected Events and Their Influence on Behavior and Cognition.
970 *Neuron* **93**, 259–280 (2017).
- 971 87. Tatz, J. R., Soh, C. & Wessel, J. R. Towards a two-stage model of action-
972 stopping: Attentional capture explains motor inhibition during early
973 stop-signal processing. *bioRxiv* 2021.02.26.433098 (2021)
974 doi:10.1101/2021.02.26.433098.
- 975 88. Diesburg, D. A. & Wessel, J. R. The Pause-then-Cancel model of human
976 action-stopping: Theoretical considerations and empirical evidence.
977 *Neurosci. Biobehav. Rev.* **129**, 17–34 (2021).
- 978 89. Jones, S. R. *et al.* Cued Spatial Attention Drives Functionally Relevant
979 Modulation of the Mu Rhythm in Primary Somatosensory Cortex. *J.*
980 *Neurosci.* **30**, 13760–13765 (2010).
- 981 90. Tan, H., Jenkinson, N. & Brown, P. Dynamic neural correlates of motor
982 error monitoring and adaptation during trial-to-trial learning. *J.*
983 *Neurosci. Off. J. Soc. Neurosci.* **34**, 5678–5688 (2014).
- 984 91. Alayrangues, J., Torrecillos, F., Jahani, A. & Malfait, N. Error-related
985 modulations of the sensorimotor post-movement and foreperiod beta-

- 986 band activities arise from distinct neural substrates and do not reflect
987 efferent signal processing. *NeuroImage* **184**, 10–24 (2019).
- 988 92. Jurkiewicz, M. T., Gaetz, W. C., Bostan, A. C. & Cheyne, D. Post-
989 movement beta rebound is generated in motor cortex: evidence from
990 neuromagnetic recordings. *NeuroImage* **32**, 1281–1289 (2006).
- 991 93. Pfurtscheller, G., Stancák, A. & Neuper, C. Post-movement beta
992 synchronization. A correlate of an idling motor area?
993 *Electroencephalogr. Clin. Neurophysiol.* **98**, 281–293 (1996).
- 994 94. Brovelli, A., Battaglini, P. P., Naranjo, J. R. & Budai, R. Medium-Range
995 Oscillatory Network and the 20-Hz Sensorimotor Induced Potential.
996 *NeuroImage* **16**, 130–141 (2002).
- 997 95. Koelewijn, T., van Schie, H. T., Bekkering, H., Oostenveld, R. & Jensen,
998 O. Motor-cortical beta oscillations are modulated by correctness of
999 observed action. *NeuroImage* **40**, 767–775 (2008).
- 1000 96. Palmer, C., Zapparoli, L. & Kilner, J. M. A New Framework to Explain
1001 Sensorimotor Beta Oscillations. *Trends Cogn. Sci.* **20**, 321–323 (2016).
- 1002 97. Fischer, P., Tan, H., Pogosyan, A. & Brown, P. High post-movement
1003 parietal low-beta power during rhythmic tapping facilitates
1004 performance in a stop task. *Eur. J. Neurosci.* **44**, 2202–2213 (2016).
- 1005 98. Schmidt, R. *et al.* Beta Oscillations in Working Memory, Executive
1006 Control of Movement and Thought, and Sensorimotor Function. *J.*
1007 *Neurosci.* **39**, 8231–8238 (2019).
- 1008 99. Pfister, R., Heinemann, A., Kiesel, A., Thomaschke, R. & Janczyk, M. Do
1009 endogenous and exogenous action control compete for perception? *J.*
1010 *Exp. Psychol. Hum. Percept. Perform.* **38**, 279–284 (2012).

- 1011 100. Hoffstaedter, F., Grefkes, C., Zilles, K. & Eickhoff, S. B. The “What” and
1012 “When” of Self-Initiated Movements. *Cereb. Cortex N. Y. NY* **23**, 520-
1013 530 (2013).
- 1014 101. Aron, A. R. From reactive to proactive and selective control: developing
1015 a richer model for stopping inappropriate responses. *Biol. Psychiatry*
1016 **69**, e55-68 (2011).
- 1017 102. Verbruggen, F. & Logan, G. D. Proactive adjustments of response
1018 strategies in the stop-signal paradigm. *J. Exp. Psychol. Hum. Percept.*
1019 *Perform.* **35**, 835-854 (2009).
- 1020 103. Shibasaki, H. Cortical activities associated with voluntary movements
1021 and involuntary movements. *Clin. Neurophysiol.* **123**, 229-243 (2012).
- 1022 104. Dockstader, C. *et al.* MEG event-related desynchronization and
1023 synchronization deficits during basic somatosensory processing in
1024 individuals with ADHD. *Behav. Brain Funct. BBF* **4**, 8 (2008).
- 1025 105. Leocani, L. *et al.* Abnormal pattern of cortical activation associated
1026 with voluntary movement in obsessive-compulsive disorder: an EEG
1027 study. *Am. J. Psychiatry* **158**, 140-142 (2001).
- 1028 106. Tzagarakis, C., Thompson, A., Rogers, R. D. & Pellizzer, G. The Degree
1029 of Modulation of Beta Band Activity During Motor Planning Is Related to
1030 Trait Impulsivity. *Front. Integr. Neurosci.* **13**, (2019).
- 1031 107. Sallard, E., Tallet, J., Thut, G., Deiber, M.-P. & Barral, J. Post-switching
1032 beta synchronization reveals concomitant sensory reafferences and
1033 active inhibition processes. *Behav. Brain Res.* **271**, 365-373 (2014).
- 1034